FULL PAPER

Adsorption and quantification of VOCs using Hybrid Magnetic Nanoparticles

María de las Nieves Piña,[a],* Paulina Rodríguez,[b] María Susana Gutiérrez,[a] David Quiñonero,[a] Jeroni Morey[a] and Antonio Frontera[a],*

Dedication ((optional))

Abstract: In this manuscript we report the ability of Fe_3O_4 magnetic nanoparticles decorated with perylene bisimides to adsorb aromatic volatile organic compounds (VOCs). We have used DFT-D3 calculations to anticipate the strong ability of the electron poor perylene bisimide to form noncovalent complexes with electron rich aromatic rings belonging to the VOC family. Subsequently, we synthesized a hybrid magnetic nanomaterial based on bisimide perylene dopamine and iron oxide nanoparticles. This material was used to fill a sorbent tube to study its ability to adsorb aromatic VOCs. We have connected two tubes in series filled with the hybrid nanoparticles. The analysis of the front and back tubes was performed by thermal desorption (TD) coupled with capillary gas chromatography (GC)/flame detector (FID). Adsorption values (defined as %VOCs found in the back tube) were determined for a series of aromatic VOCs and compared to the DFT binding energies. The tubes can be desorbed and reutilized more than 200 times without losing their properties.

Introduction

Environmental pollution is a major concern throughout the world.[1] For instance, the World Health Organization (WHO) has the water quality at the top of its priority action list. Water is vital to all forms of life and a precious resource in a wide range of industrial processes. A never-decreasing number of endogenic pollutants from agricultural, pharmaceutical, and cosmetic industries requires active monitoring.[2-4] Therefore, the development of low-cost instrumentation is imperative to have efficient tools for monitoring of water quality.[5] In this sense, the detection of volatile organic compounds (VOCs) is important due to their presence in groundwater.[6] Moreover, they are considered an essential parameter for assessing the quality of the air in

[a]   Ms. S. Gutierrez, Dra. M. N. Piña, Prof. D. Quiñonero, Prof. Dr. J. Morey and Prof. Dr. A. Frontera
      Department of Chemistry
      Universitat de les Illes Balears
      Crta. de Valldemossa km 7.5, 07122 Palma de Mallorca, Spain
      E-mail: toni.frontera@uib.es
[b]   Ms. Paulina Rodríguez
      Laboratorio de Análisis Químicos
      Dirección de Servicios Tecnológicos, Centro de Innovación Aplicada en Tecnologías Competitivas (CIATEC, A. C.)
      Omega 201, Industrial Delta, 37545 León, Guanajuato, México.

      Supporting information (calibration plots and characterization of the Fe_2O_3 nanoparticles) for this article is given via a link at the end of the document.

indoor and outdoor environments.[7-9] New sensing devices are desirable for both stand-alone operation and for developing sensor network systems. One difficult challenge is to find specific and easy to fabricate materials having high sensitivity and good selectivity to the substances to be detected.
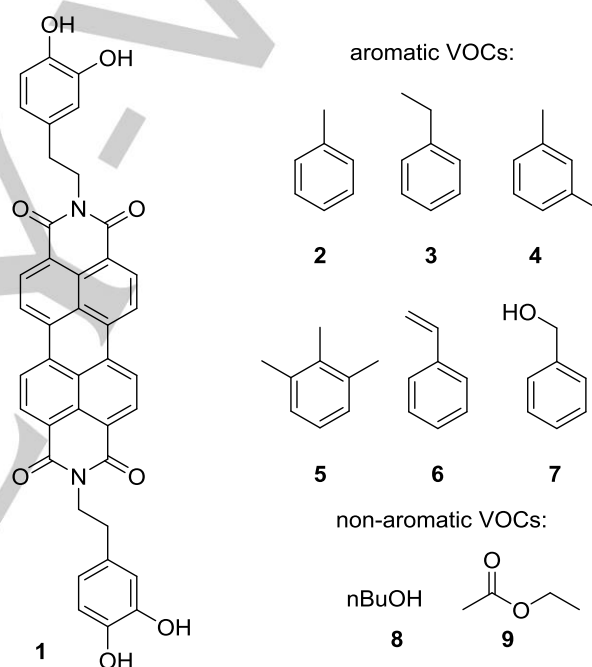
Scheme 1. Left: PBI derivative used to functionalize the Fe_3O_4NP. Right: Compounds **2** to **9** used in this study.

Selective detection is not yet accomplished in existing VOC sensing approaches.[10] This is due to the complex composition of the sampling matrices and extrinsic ambient parameters and signal degradation over time.[11] Detection using multiple sensors on the same platform improves the response due to the elimination of interferes.[11c] A convenient strategy is the integration of sensor arrays (e-noses) on a multimodal sensing platform[12] that enables accurate detection in real-time.[13] Nowadays, a variety of sensors are available (chemiresistive, optical, piezoelectric, electrochemical, etc.).[14] These sensors are of small size due to the advancements in micromachining and nanotechnology.[15] Actually, the incorporation of nanomaterial influences the sensing performance and assists in multisensing

FULL PAPER

arrays.[15-16] The utilization of different kinds of nanomaterial is gaining interest in the design of diagnostic tools, due to its advantages of higher surface-to-volume ratios, fast response and recovery times. Moreover, they are convenient to support specific detection through adequate and specific modifications of their physicochemical properties.[17] To this respect, one of the pioneering works in the use of nanostructured copolymers of polythiophene for use in VOC vapor sensors was reported by Li et al.[18] The sensing results showed new response patterns, which enhanced the discrimination of VOCs.

The magnetic nanoparticles of iron oxide (Fe_3O_4) have several advantages with respect to other materials: (i) they are easy to prepare and economic; (ii) easy to functionalize and (iii) easy to recover since they are sensitive to an external magnetic field.[19] Therefore, they are very attractive in the sense of reuse and sustainability with the environment.[19] In fact, some of us have recently described the preparation of hybrid nanoparticles formed by magnetite nanoparticles (Fe_3O_4NP) bonded to a perylene bisimide (PBI) through two dopamine or two 3-aminopropyltriethoxysilane that are adequate for the collection and removal of polyaromatic hydrocarbons (PAHs) contaminants in water for human consumption.[20]

In this study, we have used the PBI–dopamine derivative **1** (see Scheme 1) to construct hybrid nanoparticles with Fe_3O_4NP. These (PBI–dopamine)$_n$–Fe_3O_4NP hybrids were utilized for the adsorption and quantification of aromatic VOCs. We have first explored the ability of perylene bisimide to interact with aromatic VOCs via the formation of π-stacking complexes by using theoretical calculations (DFT-D3). Moreover, we have used our previous knowledge in the synthesis and characterization of these hybrid nanoparticles to build sorbent tubes filled with this material. Then an economic analytical method based on thermal desorption (TD) coupled to gas chromatography (GC) and FID detection has been developed and validated for the determination of aromatic VOCs (compounds **2–7**, see Scheme 1). The sorbent tubes were filled with perylene-based magnetic nanoparticles that showed good sensibility. Once desorbed, the filled tubes can be re-utilized more than 200 times without losing their absorption properties. Two non-aromatic VOCs (compounds **8, 9**, see scheme 1) were also compared to the aromatic VOCs. The latter showed more affinity to the hybrid nanoparticle, in agreement with DFT calculations. To the best of our knowledge, this is the first investigation reported in literature reporting the convenient utilization of Fe_3O_4 magnetic nanoparticles decorated with π-extended systems for the determination of aromatic VOCs.

Results and discussion

Preliminary MEP analysis

As a starting point we have computed the MEP (Molecular Electrostatic Potential) plotted onto de van der Waals surfaces in aromatic compounds **1** to **7** used in this study (see Figure 1). For the PBI compound **1**, the MEP values over the center of the six-membered rings are indicated. It can be observed that the MEP values are different, being the imidic ring the most positive (+13 kcal/mol). The central ring is also π-acidic (+9 kcal/mol) and finally, the rest of rings present a modest and positive potential (+3 kcal/mol). Among the aromatic VOCs, toluene and ethylbenzene present identical MEP value over the center of the ring (−21 kcal/mol) considered (compounds **2** and **3**). As the number of methyl group attached to the ring increases the MEP value over the ring becomes more negative (−23 kcal/mol for xylene **4** and −25 kcal/mol for trimethylbenzene **5**), as expected considering the electron donor ability of methyl group. Therefore, compounds **4** and **5** should have higher affinity for the (PBI–dopamine)$_n$–Fe_3O_4NP hybrid than either toluene of ethylbenzene. For styrene (**6**) the MEP value over the ring decreases due to the sp^2 nature of the vinyl substituent. However, the MEP surface also indicates that the MEP over the double bond is negative, thus suitable for contributing favorably to the π–π interaction with PBI. For benzylalcohol (**7**), the MEP over the center of the ring is also smaller in absolute value than that of toluene, thus expecting weaker π–π interactions with respect to the rest of compounds. However, the MEP value at the O atom is large (−35 kcal/mol) thus adequate for interacting with the π-acidic surface of the PBI. These preliminary results anticipate that toluene and ethylbenzene should have the weakest affinity toward the PBI functionalized magnetic NPs.
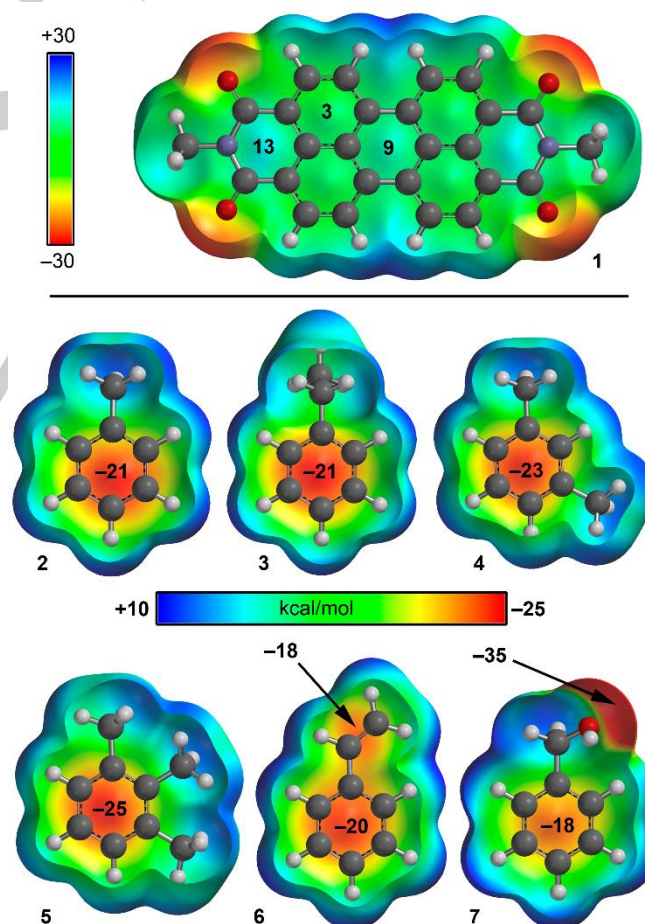

Figure 1. MEP surfaces of aromatic VOCs **2** to **7** used in the study. Energies at selected points of the surface (0.001 a.u.) are given in kcal·mol^{-1}.

FULL PAPER

Energetic study

We have also performed an energetic and geometric analysis of the complexes using DFT-D3 calculations to further study the affinity of compound **1** toward the VOCs **2–9**. We have tried different conformations and binding modes for the interaction of **1** with the VOCs. The optimized geometries of the most favorable complexes are given in Figure 2, focusing on the aromatic VOCs. In all cases we have found that π–π stacking complexes are the most favorable binding modes, with quite short equilibrium distances (3.22–3.33 Å), thus indicative of strong interaction. Moreover, in case of alkyl-substituted benzene VOCs (complexes **10–13**), several aliphatic H-atoms point to the O atoms of the PDI core, thus further contributing to the stabilization of the assemblies. The binding energies are gathered in Table 1. As anticipated by the MEP analysis, as the number of methyl substituents of benzene increases, the interaction energy becomes more favorable (from -13.7 kcal·mol^{-1} for complex **10** to -16.9 kcal·mol^{-1} for complex **13**) because the π-basicity of the ring increases and also the number of C–H···O ancillary interactions. The other two aromatic VOCs (styrene and benzyl alcohol) also present strong interaction energies (-15.1 kcal·mol^{-1} for complex **14** and -15.9 kcal·mol^{-1} for complex **15**) thus anticipating a strong affinity of the PBI functionalized nanoparticles.
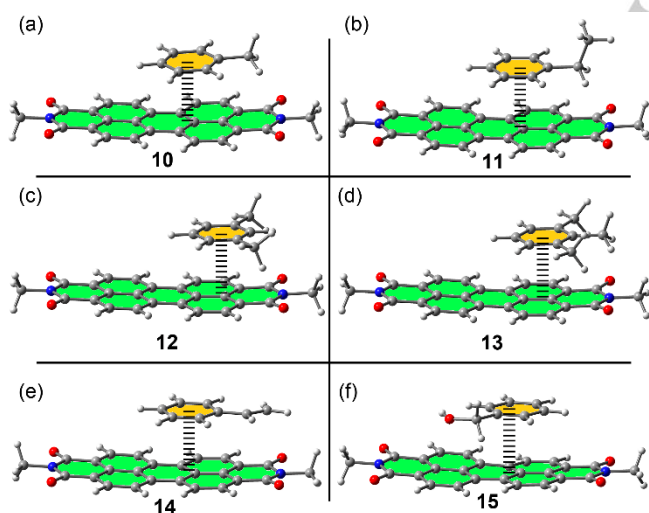

Figure 2. (a-f) Optimized geometries of 1:1 complexes **10–15** between the PBI **1** and the aromatic VOCs at the PB86-D3/def2-TZVPP level of theory.

The complexes of PBI model **1** with the non-aromatic VOCs are represented in Figure 3. Interestingly, both complexes (**16** and **17**) present similar interaction energy values and equilibrium distances. The optimized geometries are shown in Figure 3. It can be observed that the butanol complex exhibits a short lone pair (lp)–π interaction (2.87 Å) between the oxygen atom of the hydroxyl group and the central 6-membered ring of the PBI in conjunction with several C–H···π van der Waals contacts between the aliphatic H-atoms and the extended π-system.

Similarly, the ethyl acetate complex presents a short lp–π interaction between the O atom of the carbonyl group and the imidic ring. This complex is slightly less favorable than the butanol one likely due to the higher basicity of the lone pairs located in a sp^3 rather than in a sp^2 hybridized O atom. Moreover, the van der Waals contacts between alkyl chain and the PBI are more numerous in complex **16**. The interaction energies gathered in Table 1 are considerably less favorable in the non-aromatic VOCs than in the aromatic ones, therefore adsorbent material based on hybrid PBI–Fe$_3$O$_4$NPs should be more efficient for the aromatic VOCs.
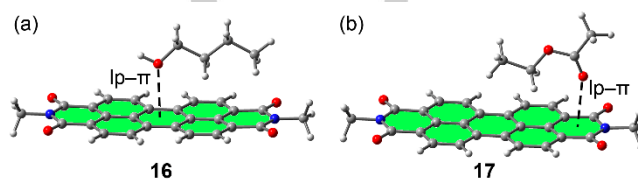

Figure 3. Optimized complexes of PBI 1 with butanol (a) and ethyl acetate (b) at the PB86-D3/def2-TZVPP level of theory.

Table 1. Interaction energies (ΔE in kcal·mol^{-1}) of complexes **10** to **17** at the PB86-D3/def2-TZVPP level of theory, equilibrium distances (R_e in Å) measured from the ring centroid of the aromatic ring to the PBI main plane in complexes **10–15** and from the O atom to the ring centroid in complexes **15** and **16** (see Figure 3). The adsorption is the percentage of VOC retained in the back tube.

Complex	ΔE (kcal·mol^{-1})	R_e^a (Å)	Adsorption
10 (1 + 2)	-13.7	3.259	75 ± 2%
11 (1 + 3)	-13.8	3.279	70 ± 4%
12 (1 + 4)	-15.2	3.276	87 ± 1%
13 (1 + 5)	-16.9	3.332	>99%[a]
14 (1 + 6)	-15.1	3.312	96 ± 2%
15 (1 + 7)	-15.9	3.263	97 ± 1%
16 (1 + 8)	-10.0	2.873	94 ± 3%
17 (1 + 9)	-9.3	2.838	67 ± 2%

[a]The presence of VOC was not detected in the front tube.

Synthesis of the nanoparticles, fabrication of the sorbent tubes and adsorption-desorption experiments

We have followed the methodology recently developed by some of us for the preparation of the hybrid nanoparticles. Briefly, the perylene bisimide-dopamine ligand, PBI-DA, was synthesized in good yield (90%) by adding two equivalents of dopamine hydrochloride to one equivalent of perylene-3,4,9,10-tetracarboxylic dianhydride in water. Subsequently, the conjugation of the PBI-DA ligand with the magnetite –prepared by the classical coprecipitation method from Fe(II) and Fe(III) iron

FULL PAPER

salts– was carried out using the microwave-assisted heating method[21] since it increases significantly the covalent functionalization of the nanoparticle.[21] We have prepared the sorbent tubes (see Figure 4A) by using polyethylene tubes of 6 mm of diameter and 90 mm of length that were filled with 450 mg of hybrid nanoparticles and unsilanized glass wool was put at both ends.

We have studied the capability of sorbent tubes filled with hybrid Fe_3O_4NPs to collect the aromatic and non-aromatic VOCs described above. Initially, we have used one tube for the generation of the calibration plots, as schematically represented in Figure 4B. The standard solutions were freshly prepared. For the doping of the tubes we used the commercial doping device that allows the manual injection of the VOC through a Swagelock adapter that connects the tube without any possibility of leakage. The N_2 flow ensures the homogeneity of the sample through the sorbent. For the sake of reproducibility, we have always used 1 µl of VOC solution and a doping time of 5 min (see experimental methods for details). After the doping, a desorption is performed at 300 °C during 10 min and the VOC that was previously adsorbed in the tube is concentrated in a criofocusing trap at -30 °C. Afterwards, the trap is quickly heated from -30 °C to 300 °C and the VOC is sent to the gas chromatograph and finally injected through a line at 200 °C. The analysis of the data allows the generation of the calibration plots and to know the working range of concentrations (see ESI for details).
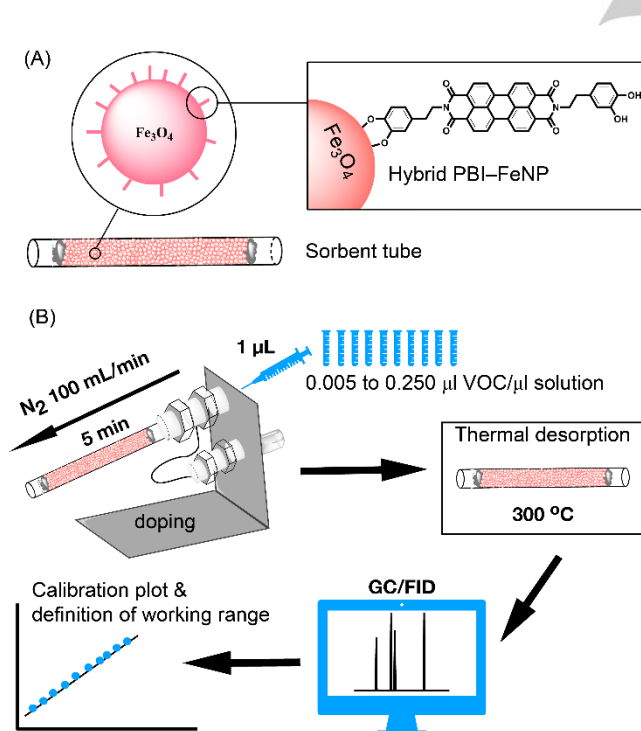
To investigate the relative ability of the hybrid nanoparticles to interact with the aromatic VOCs, we have performed additional investigations using two sorbent tubes connected in series (using a Swagelock–PFA union) as represented in Figure 5. Each tube was filled with 450 mg of hybrid nanoparticles, and we periodically checked that both tubes were able to give the same result. After thermal cleaning (see experimental methods) we were able to reuse the tubes >200 times without any loss of their adsorption properties. For each experiment, we have injected a known quantity of VOC (0.27 to 0.41 mg) that is larger than the upper limit of the working range used for the generation of the calibration plots. The individual analysis of the front tube allows to measure the quantity of VOC that has not been adsorbed in the back tube. The results given as % VOC in the back tube are gathered in Table 1 and the absolute values are given in Table 2.

At this point it should be mentioned that we have performed the same experiments using tubes filled with the non-functionalized magnetic NP (without the PBI unit). As a result, the adsorption capability of the NP decreases drastically, ranging from 40 to 60% of adsorption reduction. Moreover, no significant differences were observed for the adsorption capacity of the magnetic NP for the different aromatic VOCs, thus supporting the differential feature and crucial role of the PBI unit in the hybrid NPs interacting with the VOCs, as further discussed below.
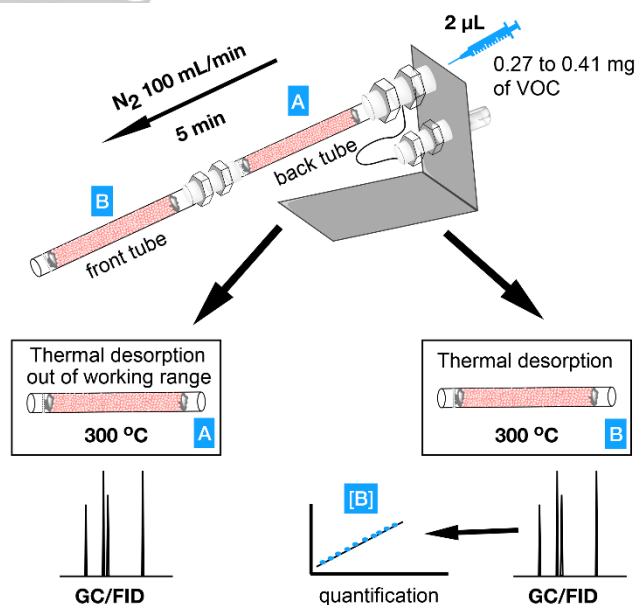

Figure 5. Schematic representation of the tubes connected in series. The quantitative analysis of front tube (B) allows to quantify the amount of VOC adsorbed in the back tube (A).

Figure 4. (A) Schematic representation of the sorbent tube. (B) Methodology used to perform the calibration plots and to define the working range.

FULL PAPER

Table 1. Retention times (min), milligrams of injected VOC, milligrams of VOC in the back tube

VOC	RT (min)	Injected VOC (mg)	VOC in tube B[a] (mg)
2	17.4	0.35	0.087 ± 0.005
3	20.6	0.35	0.104 ± 0.015
4	20.8	0.34	0.044 ± 0.004
5	25.9	0.35	0.000[b]
6	21.7	0.36	0.019 ± 0.008
7	27.6	0.27	0.007 ± 0.001
8	14.5	0.32	0.018 ± 0.008
9	12.1	0.41	0.136 ± 0.006

[a]Data from three independent experiments. [b]Under the limit of detection

The comparison of the interaction energies obtained for the PBI···VOC complexes **10**–**17** and the % VOC found in the back tube provides some hints regarding the binding mode of the VOCs and the hybrid nanoparticles. Quite remarkably, if we consider the aromatic VOCs **2**–**5** where the benzene is substituted with aliphatic groups, the adsorption ability of the hybrid nanoparticles increases as the number of substituents increases. That is, the %VOC is 71-75% in monosubstituted toluene and ethyl benzene to 87% in *m*-xylene and finally 100% in trimethylbenzene. This strongly agrees with the increase in the π-basicity of the aromatic ring and, more importantly, with the interaction energies of the π-stacked complexes **10**–**13**. Therefore, it is observed a correlation between the experimental % VOC retained in the back tube and the strength of the π–π stacking interactions between the PBI and the VOC, thus supporting the proposed mechanism of interaction. Regarding the styrene and benzyl alcohol, there is a reasonable agreement between the interaction energy and the retention percentage. It is also worth mentioning that ethyl acetate exhibits the lowest percentage of retention and its binding energy is considerably smaller than that obtained for aromatic VOCs, thus confirming the higher ability of the hybrid nanoparticle to interact with aromatic VOCs. Unexpectedly, this is not confirmed for butanol that exhibits a large percentage of adsorption. Since the interaction energy with the π-system of the PBI is modest (see Table 1), we hypothesize that in this case the binding mechanism is different. Actually, due to the presence of the OH group in butanol, it can form strong H-bonding interactions with the phenol groups of the catechol ring, thus explaining its high adsorption value determined experimentally.

Conclusions

In conclusion, we have shown the ability of Fe_3O_4 magnetic nanoparticles covalently bonded to perylene bisimides via dopamine linkers to adsorb aromatic VOCs. We have also carried out DFT-D3 calculations to analyze the binding mode and we

have been able to correlate the interaction energies of some π–π stacking complexes of PBI with a series of aromatic VOCs with the adsorption capacity of the hybrid nanoparticles measured experimentally. We have utilized a set-up where two tubes filled with nanomaterial are connected in series. We have measured the %VOCs retained in the back tube after the injection of a known amount of VOC in the back tube and analyzed the VOC present in the front tube.

This investigation also demonstrates that this hybrid material can be used for the construction of sorbent tubes and utilized for the quantification of aromatic VOCs. The tubes can be desorbed and reutilized more than 200 times without losing their properties. Since this material is also able to adsorb butanol efficiently, we are currently performing further investigations in nonaromatic VOCs to expand applicability of the method in other families of VOCs.

Experimental and theoretical methods

The synthesis and characterization of the nanoparticles used in this work have been previously described by us.[19] The nanoparticles are thermally stable up to 450 °C, therefore they are suitable for utilization in the experiments detailed below, since the maximum temperature used in the different apparatus is 375°C. We have not detected any degradation of the magnetic nanoparticles even after 200 repetition of the experiment. The VOC analytes were purchased from Sigma-Aldrich and Fluka (Buchs, Switzerland) and their purity was higher than 98% in all cases. The solvent was purchased from Scharlau (chromatographic quality). The polyethylene tubes (6 mm of diameter and 90 mm length) and the unsilanized glass wool were purchased from Supelco (Bellefonte, PA, USA).

Standard solutions. Stock standard solutions for each VOC were freshly prepared on the day of use and stored at 4 °C in darkness in 1.5 ml flask. These mother solutions were further diluted in MeOH to prepare standard solutions: 0.005, 0.010, 0.015, 0.020, 0.030, 0.050, 0.100, 0.150, 0.200 and 0.250 µl VOC/µl, and a final volume of 500 µl.

Tubes filled with hybrid nanoparticles We have used one tube for the generation of the calibration plots and two tubes connected in series to determine the percentage of retention of the analyte in the functionalized nanoparticles. Each tube was filled with 450 mg of hybrid nanoparticles and periodically, we checked that both tubes were able to give the same results when doped with the same quantity of a given VOC. After total desorption, we also checked that both tubes were perfectly clean. Before the first use, tubes were conditioned by thermal cleaning (250 °C for 20 min, 300 °C for 20 min, 330 °C for 20 min, 350 °C for 20 min and 375 °C for 20 min) under a flow rate of dry N_2 of 70 ml min⁻¹. For subsequent uses, pre-conditioning at 375 °C for 20 min was applied. After conditioning, they were immediately sealed with Swagelock end caps fitted with PTFE ferrules and stored in closed plastic boxes filled with desiccant material. Samples were freshly prepared and only few seconds after the preparation of the tubes (doping and subsequent desorption). For the doping of the tubes we used the commercial doping device supplied by the instrument manufacturer. This device allows the manual injection (under a flow rate of dry N_2 of 100 ml min⁻¹) of the VOC through a Swagelock adapter (stainless steel) that connects the tube without any possibility of leakage. The N_2 flow ensures the homogeneity of the sample through the sorbent. For the sake of reproducibility, we have always used 1 µl of VOC solution

FULL PAPER

and a doping time of 5 min and during the first minute the syringe was kept in the injector in order to maintain the flux unperturbed.

Analytical instrumentation and procedure. The VOC analyses were carried out using a manual injection (Unity 2 model, Markes) thermal desorption (TD) coupled to a gas chromatograph with a FID detector (6890A model, Agilent Technologies). The first step is an initial pre-desorption during 0.1 min and a flux of 20 mL/min. Subsequently, a primary desorption is performed at 300 °C during 10 min, with a split of 4 mL/min. During this time period, the analyte that was previously adsorbed in the tube is concentrated in a criofocusing trap that contains 30 mg of Tenax TA, and kept at -30 °C. Afterwards, the trap is quickly heated from -30 °C to 300 °C and kept at the final temperature during 10 min and, thus, the secondary desorption takes place. In this step the analyte is sent to the gas chromatograph using a split with a flux of 7 mL/min and finally injected to a capillary column (DB-624, 60m x 0.25mm x 1.4 μm, Agilent Technologies) through a line at 200 °C. The oven temperature was initially set at 40 °C during 1 min and progressively increased (rate of 6 °C/min) until 230 °C. This final temperature is maintained during 5 min. The carrier gas was premium quality N_2 with a flux of 1 mL/min approximately.

Theoretical details. The energies of all complexes included in this study were computed at the BP86-D3/def2-TZVPP level of theory. We have used the BP86 functional with the latest available correction for dispersion (D3),[22] since it is needed to describe adequately the π-stacking interactions. The calculations have been performed by using the program TURBOMOLE version 7.0.[23] The MEP surfaces were computed using the Spartan'10 software[24] at the B3LYP/6-31+G* and the van der Waals surface.

Acknowledgements

References

[1]   M. Sowden, U. Mueller, D. Blake, *Atmos. Environ.* **2018**, *183*, 154-164 and references cited therein.
[2]   M. Sarker B. M. Bhadra P. W. Seo, S. H. Jhung, *J. Hazardous Mat.* **2017**, *324*, 131–138.
[3]   M. Yasukawa, S. Mishima, M. Shibuya, D. Saeki, T. Takahashi, T. Miyoshi, H. Matsuyama, *J. Membrane Sci.* **2015**, *487*, 51–59.
[4]   M. Shestakova, M. Sillanpää, *Chemosphere* **2013**, *93*, 1258–1267.
[5]   E. S. Snow, F. K. Perkins, E. J. Houser, S. C. Badescu, T. L. Reinecke, *Science* **2005**, *307*, 1942-1945.
[6]   I. Azzouz, Y. G. Habba, M. Capochichi-Gnambodoe, F. Marty, J. Vial, Y. Leprince-Wang, T. Bourouina, *Microsyst. Nanoeng* **2018**, *4*, 17093.
[7]   A. Ribes, G. Carrera, E. Gallego, X. Roca, M. J. Berenguer, X. Guardino, J. *Chromatography A* **2007**, *1140*, 44–55.
[8]   G. Churkina, F. Kuik, B. Bonn, A. Lauer, R. Grote, K. Tomiak, T. M. Butler, *Environ. Sci. Technol.* **2017**, *51*, 6120–6130.
[9]   B. Bonn, J. Kreuzwieser, F. Sander, R. Yousefpour, T. Baggio, O. Adewale, *Climate* **2017**, *5*, 78.
[10]   A. H. Jalal, F. Alam, S. Roychoudhury, Y. Umasankar, N. Pala, S. Bhansali, *ACS Sens.*, **2018**, *3*, DOI: 10.1021/acssensors.8b00400.
[11]   (a) Y. Paska, H. Haick, *ACS Appl. Mater. Interfaces* **2012**, *4*, 2604– 2617. (b) A. H. Jalal, Y. Umasankar, P. J. Gonzalez, A. Alfonso, S. Bhansali, *Biosens. Bioelectron.* **2017**, *87*, 522–530. (c) A. Romain, J. Nicolas, M. Pardo, G. Sberveglieri, *AIP Conf. Proc.* **2009**, *1137*, 443.
[12]   J. Dieffenderfer, H. Goodell, S. Mills, M. McKnight, S. Yao, F. Lin, E. Beppler, B. Bent, B. Lee, V. Misra, Y. Zhu, O. Oralkan, J. Strohmaier, J. Muth, D. Peden, A. Bozkurt, *IEEE J. Biomed Health Inform.* **2016**, *20*, 1251– 1264.
[13]   S. Yao, P. Swetha, Y. Zhu, *Adv. Healthcare Mater.* **2018**, *7*, 1700889.
[14]   R. A. Kadir, R. A. Rani, A. S. Zoolfakar, J. Z. Ou, M. Shafiei, W. Wlodarski, K. Kalantar-zadeh, *Sens. Actuators, B* **2014**, *202*, 74–82. (b) H.-J. Kim, J.-H. Lee, *Sens. Actuators, B* **2014**, *192*, 607–627. (c) J. Devkota, P. R. Ohodnicki, D. W. Greve, *Sensors* **2017**, *17*, 801. (d) V. Semwal, A. M. Shrivastav, R. Verma, B. D. Gupta, *Sens. Actuators, B* **2016**, *230*, 485–492. A. H. Jalal, Y. Umasankar, S. Bhansali, *ECS Trans.* **2016**, *72*, 25–31.
[15]   N.-H. Kim, S.-J. Choi, D.-J. Yang, J. Bae, J. Park, I.-D. Kim, *Sens. Actuators, B* **2014**, *193*, 574−581.
[16]   R. Vishinkin, H. Haick, *Small* **2015**, *11*, 6142−6164.
[17]   Y. Y. Broza, H. Haick, *Nanomedicine*, **2013**, *8*, 785−806.
[18]   B. Li, G. Sauvé, M. C. Iovu, M. Jeffries-EL, R. Zhang, J. Cooper, S. Santhanam, L. Schultz, J. C. Revelill, A. G. Kusne, T. Kowalewski, J. L. Snyder, L. E. Weiss, G. K. Fedder, R. D. McCullough, D. N. Lambeth, *Nano Lett.* **2006**, *6*, 1598-1602.
[19]   K. A. López, M. N. Piña, D. Quiñonero, P. Ballester, J. Morey, *J. Mater. Chem. A* **2014**, *2*, 8796-8803.
[20]   M. S. Gutiérrez, P. Duel, F. Hierro, J. Morey, M. N. Piña, *Small* **2018**, *14*. 1702573.
[21]   M. S. Gutiérrez, M. N. Piña, J. Morey, *RSC Adv.* **2017**, *7*, 19385-19390.
[22]   S. Grimme, J. Antony, S. Ehrlich, H. Krieg, *J. Chem. Phys.* **2010**, *132*, 154104-19.
[23]   R. Ahlrichs, M. Bär, M. Hacer, H. Horn, C. Kömel, *Chem. Phys. Lett.* **1989**, *162*, 165–169.[24]   Spartan'10 v1.10, Wavefunction Inc, Irvine, CA, USA.

FULL PAPER

Entry for the Table of Contents

FULL PAPER

In this manuscript we report the ability of Fe_3O_4 magnetic nanoparticles decorated with perylene bisimides to adsorb aromatic volatile organic compounds (VOCs). We have also carried out DFT-D3 calculations to anticipate the strong ability of the electron poor perylene bisimide to form noncovalent complexes with electron rich aromatic rings belonging to the VOC family.

Hybrid PBI–FeNP

Fe_3O_4

sorbent tube
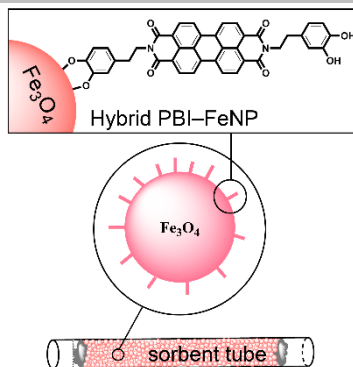
M. N. Piña, P. Rodríguez, M. S. Gutiérrez, D. Quiñonero, J. Morey and A. Frontera

Page No. – Page No.

Adsorption and quantification of VOCs using Hybrid Magnetic Nanoparticles .